Optimization of the Antitumor Activity of Sequence-specific Pyrrolobenzodiazepine Derivatives Based on their Affinity for ABC Transporters

The AAPS Journal, Vol. 12, No. 4, December 2010 (© 2010)
DOI: 10.1208/s12248-010-9225-x

Research Article

Optimization of the Antitumor Activity of Sequence-specific Pyrrolobenzodiazepine Derivatives Based on their Affinity for ABC Transporters

Maciej Kaliszczak,[1,4,7] Dyeison Antonow,[2] Katan I. Patel,[1] Philip Howard,[2] Duncan I. Jodrell,[1,5] David E. Thurston,[2,3] and Sylvie M. Guichard[1,6]

Received 27 May 2010; accepted 15 July 2010; published online 12 August 2010

Abstract. Pyrrolobenzodiazepine (PBD) derivatives are highly potent sequence-specific DNA cross-linking agents. The present study aimed to identify key physicochemical properties influencing the interaction of a series of PBDs (four dimers and 12 monomers) with the three major human ATP-binding cassette (ABC) transporters (P-gp, ABCG2, and MRP1). Isogenic cell lines expressing P-gp and ABCG2, cell lines with acquired resistance to cytotoxic agents due to the high expression of ABC transporters, and specific inhibitors against P-gp, ABCG2, and MRP1 were used. P-gp and ABCG2 decreased the permeability of the PBD dimers across cell membranes and their interaction with DNA, reducing DNA damage and the overall cytotoxic effect. PBD monomer SG-2823 formed a conjugate with glutathione and interacted with MRP1, reducing its cytotoxic effect in A549 cells. Structure–activity relationship revealed that the interaction of PBDs with the transporters could be predicted considering the molecular weight, the lipophilicity, the number of (N+O) atoms and aromatic rings, the polar surface area, the hydrogen bonding energy, and electrophilic centers. A rational design of novel PBDs with increased potency and reduced interaction with the ABC transporters is proposed.

KEY WORDS: ABCG2; glutathione; MRP1; P-glycoprotein; structure–activity relationship.

INTRODUCTION

Cellular resistance is considered to be a major cause of failure of chemotherapy treatment in patients with cancer (1,2). Resistance mechanisms can be divided in two main groups. The first group includes factors altering the drug disposition of anticancer agents, modifying their pharmacokinetic or the drugs access to certain areas of the body (blood brain barrier for example) (3); the second group includes factors altering the antitumor effects of drugs (4). ABC transporters form a superfamily of proteins implicated in both groups of resistance mechanisms. Three major ABC transporters have been studied: P-gp also termed multidrug resistance 1 (MDR1) or ABCB1, ABCC1 commonly referred as multidrug resistance protein 1 (MRP1) and ABCG2 also named breast cancer resistance protein. These transporters form large tridimensional structures spanning the cell membrane and exclude endogenous and exogenous chemical entities from the cell in an ATP-dependent fashion. Genetic polymorphisms of both ABCB1 and ABCG2 have been correlated with alterations of pharmacokinetics of anticancer agents and other therapeutics (3). However, ABC transporters have mainly been studied for their overexpression in multiple tumor types leading to multidrug resistance (MDR), thereby decreasing the intracellular concentrations of anticancer agents or increasing their detoxification by cancer cells.

A wide variety of drugs, structurally dissimilar and belonging to various therapeutic classes interact with ABC transporters. However, for specific therapeutic classes with low therapeutic indexes such as anticancer drugs, HIV-protein inhibitors, antibiotics, or immunosuppressants, the impact of drug transporters may have significant consequences (1). As part of the drug discovery activities, it is, therefore, key to minimize the interaction of compounds with ABC transporters to optimize both their pharmacokinetic and their biological activity. Understanding of parameters controlling these interactions is crucial for drug optimization.

SJG-136 is a pyrrolo[2,1-*c*][1,4]benzodiazepine (PBD) dimer forming DNA crosslinks spanning six base pairs with a

Electronic supplementary material The online version of this article (doi:10.1208/s12248-010-9225-x) contains supplementary material, which is available to authorized users.

[1] Cancer Research UK Pharmacology and Drug Development Group, University of Edinburgh Cancer Research Centre, Crewe Road, Edinburgh, UK.
[2] Spirogen Ltd, 2 Royal College Street, London, NW1 0NH, UK.
[3] Cancer Research UK Gene Targeted Drug Design Research Group, The School of Pharmacy, University of London, 29-39 Brunswick Square, London, WC1N 1AX, UK.
[4] Division of Surgery, Oncology, Reproductive Biology and Anaesthetics, Imperial College, Hammersmith Hospital, Du Cane Road, London, W12 0NN, UK.
[5] CRUK Cambridge Research Institute, University of Cambridge, Li Ka Shing Centre, Robinson Way, Cambridge, UK.
[6] AstraZeneca, Mereside, Alderley Park, Macclesfield, Cheshire, UK.
[7] To whom correspondence should be addressed. (e-mail: m.kaliszczak@imperial.ac.uk)

preference for purine-GATC-pyrimidine sequences (5–7). SJG-136 is extremely potent and showed cytotoxic effects at nM concentrations in a broad variety of tumor types *in vitro* and antitumor effects in xenograft models *in vivo* (5,8). SJG-136 is a P-gp substrate, which reduces its cytotoxic effect in cancer cells expressing high levels of P-gp (9). PBD monomers have shown significant cytotoxic effects *in vitro* in a number of tumor types despite the absence of crosslinks formation and preclinical studies have highlighted the potency of the PBD monomers in a number of tumor types (10–12). However, their interaction with ABC transporters is unknown. SJG-136 is the first PBD to enter clinical development and is currently being assessed in Phase II clinical trials (5,7,13).

This study evaluates the interactions of both PBD dimers and monomers with ABC transporters P-gp, MRP1, and ABCG2 and presents a strategy to optimize further this promising class of anticancer agents.

MATERIALS AND METHODS

Materials

The PBD derivatives were synthesized through multiple step synthesis that has been described in full elsewhere (10,14,15). Aliquots were obtained from Spirogen Ltd (London, UK). MK-571 was obtained from (BioMol International, Exeter, UK). Transwell plates with polyethylene terephthalate membrane (Millicell 24) were obtained from Millipore (Watford, UK). Hanks buffer balanced saline (HBSS) was obtained from Fisher/Thermo Scientific HyClone (Cramlington, UK). Lucifer yellow was obtained from Molecular Probes (Invitrogen, Paisley, UK). All other chemicals were obtained from Sigma–Aldrich (Poole, UK). Phospho-histone H2AX (Ser 139) rabbit antibody was obtained from cell signaling (New England Biolabs, Hitchin, UK). Goat anti-rabbit FITC-conjugated was obtained from Abcam (Cambridge, UK).

Cell Culture

Adenocarcinoma cell line Caco-2, colon cancer cell lines HCT 116, HCT-15, and lung cancer cell line A549 were obtained from the American Type Cell Culture Collection (Rockville, Maryland) and European Collection of Cell Cultures (Salisbury, UK). Ovarian cancer cell line A2780 and drug resistant sub-clones A2780^{AD} were provided by the National Cancer Institute (Bethesda, Maryland). Murine fibroblasts (3T3 GP+E86) and 3T3 transfected with c-DNA expressing P-gp were kindly provided by Dr. E. Schuetz from St. Jude's Children Research Hospital (Memphis, Tennessee). Breast cancer cell line MDA-MB-231 transfected with an empty vector (MDA-MB-231/V8) and MDA-MB-231 transfected with c-DNA expressing ABCG2 (MDA-MB-231/R12) were kindly provided by Dr. D. Ross from the University of Maryland (Baltimore, Maryland). Breast cancer cell line MCF7 and mitoxantrone (MX)-resistant sub-clones MCF7-MX were kindly provided by Dr. E. Schneider from the University of Maryland (Baltimore, Maryland).

HCT 116, HCT-15, A2780, and A2780^{AD} were grown in monolayer in RPMI 1640 medium supplemented with 5% *v/v* fetal calf serum (FCS). 3T3 GP+E86, A549, MCF7, and MDA-MB-231 cells were grown in Dulbecco's modified Eagle's medium (DMEM) supplemented with 10% FCS. Caco-2 cells were grown in DMEM with a high glucose content (4.5 g/L) supplemented with 10% FCS. A2780^{AD} cells are derived from the parental A2780 cell line and are resistant to doxorubicin. They were obtained by stepwise incubation of increasing concentration of doxorubicin (16). They were maintained in 10^{-7} M doxorubucin and were drug-free 1 week prior to any experiment. MCF7-MX cells are derived from the parental MCF7 cell line and are resistant to mitoxantrone. They were obtained by stepwise incubation of increasing concentration of mitoxantrone (17). They were maintained in 10^{-8} M mitoxantrone and were drug-free 1 week prior to any experiment. MDA-MB-231 cells were maintained in 1 mg/mL of G418 sulfate and were antibiotic-free 1 week prior to any experiment. All cells were tested regularly for mycoplasma contamination and were mycoplasma-free for the period of the study.

Cytotoxicity Assay

Drug concentrations that inhibited 50% of cell growth (GI_{50}) were determined using a sulforhodamine B technique as described elsewhere (18). All cell lines were treated for 24 h on day 2 and allow growing for an additional 3 days. When cells were pretreated with different inhibitors (50 μM MK-571, 10 μM Fumitremorgin C, 100 μM dicumarol), cells were treated 1 h before drug exposure (24 h prior to the experiment for L-buthionine–sulfoximine, 10 μM). Optical densities were measured at 540 nm with a Biohit BP-800 (Bio-Hit, Helsinki, Finland). Growth inhibition curves were plotted as percentage of control cells, and GI_{50} values were determined by Graphpad Prism 4 Software (San Diego, California) by fitting a sigmoidal curve with variable slope.

Immunostaining for γ-H2AX

Exponentially growing A2780^{AD} cells were seeded in chamber slides on day 1. The cells were treated on day 3 with 10 nM of DRG-16 for 24 h. When cells were pretreated with verapamil, they were treated with 5 μg/mL verapamil starting 1 h before drug exposure. Cells were washed in PBS and then incubated in 2% paraformaldehyde in PBS for 10 min, washed in PBS, permeabilized in 0.1% triton X100, diluted in PBS at room temperature (RT) for 10 min, washed, blocked with PBS containing 1% bovine serum albumin, and incubated overnight at 4°C with an anti-phosphohistone H2AX antibody, washed, incubated with a FITC, AlexaFluor 488-conjugated goat anti-mouse IgG antibody for 1 h at RT, and washed in PBS. Slides were mounted and visualized with a Leitz Laborlux UV microscope (Wetzlar, Germany) using a ×40 objective fitted with a Spot Insight 4 camera (Diagnostic Instruments, Sterling Heights, Michigan). The intensity of fluorescence was evaluated with Photoshop CS3 (Adobe Systems Incorporated, San Jose, California).

Transwell Assay

Caco-2 cells were seeded on to cell culture chambers (transwells) for 21 days, and the media changed every other day. The transepithelial electric resistance was measured

using an epithelial voltohmmeter equipped with an STX2 electrode (World Precision Instruments, Sarasota, Florida), and it was verified to be >300 Ω/cm^2 prior to all experiments. The assay was started by replacing the culture medium with HBSS containing 1 μM of drug. The plates were placed on an orbital shaker (60 rpm) during the experiment. After 2 h, a volume of 10 μL of each chamber was collected for analysis by LC/MS. The permeability of a test compound was defined by the following equation (Eq. 1) (19):

$$Papp = (dQ/dt)/AC_0 \quad (1)$$

Where A is the surface area of the transwell membrane, C_0 is the molar drug concentration in the donor chamber at time and dQ/dt is the rate of transfer of the compound to the receiver chamber, determined from the slope of the graph concentration (dQ) *versus* time (dt).

It has been stated that if a compound exerts a ratio between the secretion (permeability from the basal to the apical side ($Papp_{B\rightarrow A}$)) and the absorption (permeability from the apical to the basal side ($Papp_{A\rightarrow B}$))>3, it can be considered as being actively effluxed (20). At the end of the assay, the integrity of the monolayer was verified by measuring the amount of lucifer yellow, a fluorophore, which has passed through the membrane using a plate reader (Wallac EnVision reader, PerkinElmer, Massachusetts) and verified to be <2% of the concentration in the donor chamber (21,22). The integrity of the monolayer was assessed post-drug transport as lucifer yellow may interfere with LC/MS analysis.

Detection of Glutathione-Conjugated SG-2823

SG-2823 (10 μM) was incubated with GSH (1 mM) for 15 min at RT in cell-free HBSS. The products of the reaction were analyzed by LC/MS. The HPLC system comprised of a Dionex 3000 Ultimate series LC (Sunnyvale, California) connected to a 4000 Q Trap LC-MS/MS system (Applied Biosystems, Foster City, California), equipped with an orthogonal electrospray ion source. Data were acquired and processed with Chromeleon 6.1 (Dionex, Sunnyvale, California) and Analyst 1.4 chromatography manager software (Applied Biosystems, Foster City, California). Compounds were separated on a Dionex Acclaim® C16 (150×2.0 mm I.D.) and 3 μm particle size column protected by a Phenomenex Gemini® C18 (4.0×2.0 mm I.D.) and 3 μm particle size guard cartridge (Phenomenex, Torrance, California). The HPLC method used gradient elution; mobile phase solvent A was water with 0.1% formic acid, and mobile phase B was acetonitrile with 0.1% formic acid. The initial mobile phase composition of 99% solvent A and 1% solvent B was maintained for 3 min. Between 3 and 9 min, the percentage of mobile phase B was increased to 75%, kept constant for 2 min, and then back to the initial mobile phase composition within 2 min, with a total run time of 16 min. The column was set at a flow rate of 0.23 mL/min and a temperature of 33°C. A sample volume of 6 μL was used for all LCMS experiments. The mass spectrometer was operated in electrospray mode. The source temperature was 450°C, and the spray voltage of 3 kV was used. The collision gas pressure was 1.5 mTorr. All analytes were optimized using the Analyst software auto tune facility for SRM transitions with dwell times set at 75 ms.

Analysis of the Hydrogen Bond Acceptor Patterns

The three-dimensional structures of compounds were modeled with a modified version of Allinger's MM2 force field approach, using the software Chem3D (Cambridge Soft Corporation, Cambridge, Massachusetts) (23). The chemical structures were then screened for electron donor groups (i.e., O, N, S). The spatial distance between neighboring atoms carrying the free electron pair was measured. The hydrogen bond acceptor pattern was determined and quantified as formed either by two electron donor groups separated by a spatial distance of 2.5±0.3 Å or two electron donor groups separated by 4.6±0.6 Å or three electron donor groups separated by 4.6±0.6 Å, as described by Seelig *et al.* (24). In order to quantify the hydrogen bond acceptor pattern, relative hydrogen bond energy units were assigned: an oxygen-containing electron donor group equal 1 while a weaker oxygen-free electron donor group was 0.5 (24).

Determination of LogP, PSA, and Partial Charge

The hydrophobicity of the molecules, Log*P,* the polar surface area (PSA), defined by as a sum of surfaces of polar atoms (usually oxygen, nitrogen, and attached hydrogen), and the partial charge (measured by the extended Hückel calculation) were also determined using Chem3D.

Surface Activity

Experiments were carried out as previously described (25). Water used for buffers and solutions was nanopure with a resistivity of 17.5 MΩ/cm. Tris buffer (50 mM, containing 114 mM NaCl) was adjusted with HCl to the desired pH of 7.4. The surface pressure was measured at 23±1°C using a teflon trough (3–5 mL filling volume, Nima Technology Ltd, Coventry, UK) and a Wilhelmy plate covered by a plexiglas hood to minimize evaporation and using drug concentrations ranging from 10^{-4} to 10^{-6} M. DMSO, used as a solvent, was tested to correct for its own surface activity. The measurements were monitored using a DST9005 tensiometer (Nima Technology Ltd, Coventry, UK).

RESULTS

P-gp and ABCG2 Decreases the Growth Inhibitory Effect of PBD Dimers

The potential interactions of PBD dimers with ABC transporters P-gp and ABCG2 was assessed using isogenic cell lines expressing the cDNA for the respective transporters. The growth inhibitory effect of four PBD dimers SJG-136, DSB-120, DRG-16, and ELB-21 (Fig. 1a) was determined in 3T3 cells expressing an empty vector (3T3 GP+E86) or the cDNA of P-gp (pHamdr1) and MDA-MB-231 expressing vector control (V8) or the cDNA of ABCG2 (R12). In the P-gp overexpressing set of cell lines, the ratio of GI_{50}s ranged from 33 to 46 (Fig. 2a). In MBD-MB-231/V8 and R12, the ratio of GI_{50}s ranged from 3.4 to 4.1 (Fig. 2b). These results suggest that overexpression of P-gp or ABCG2 impairs the cytotoxic effect of PBD dimers.

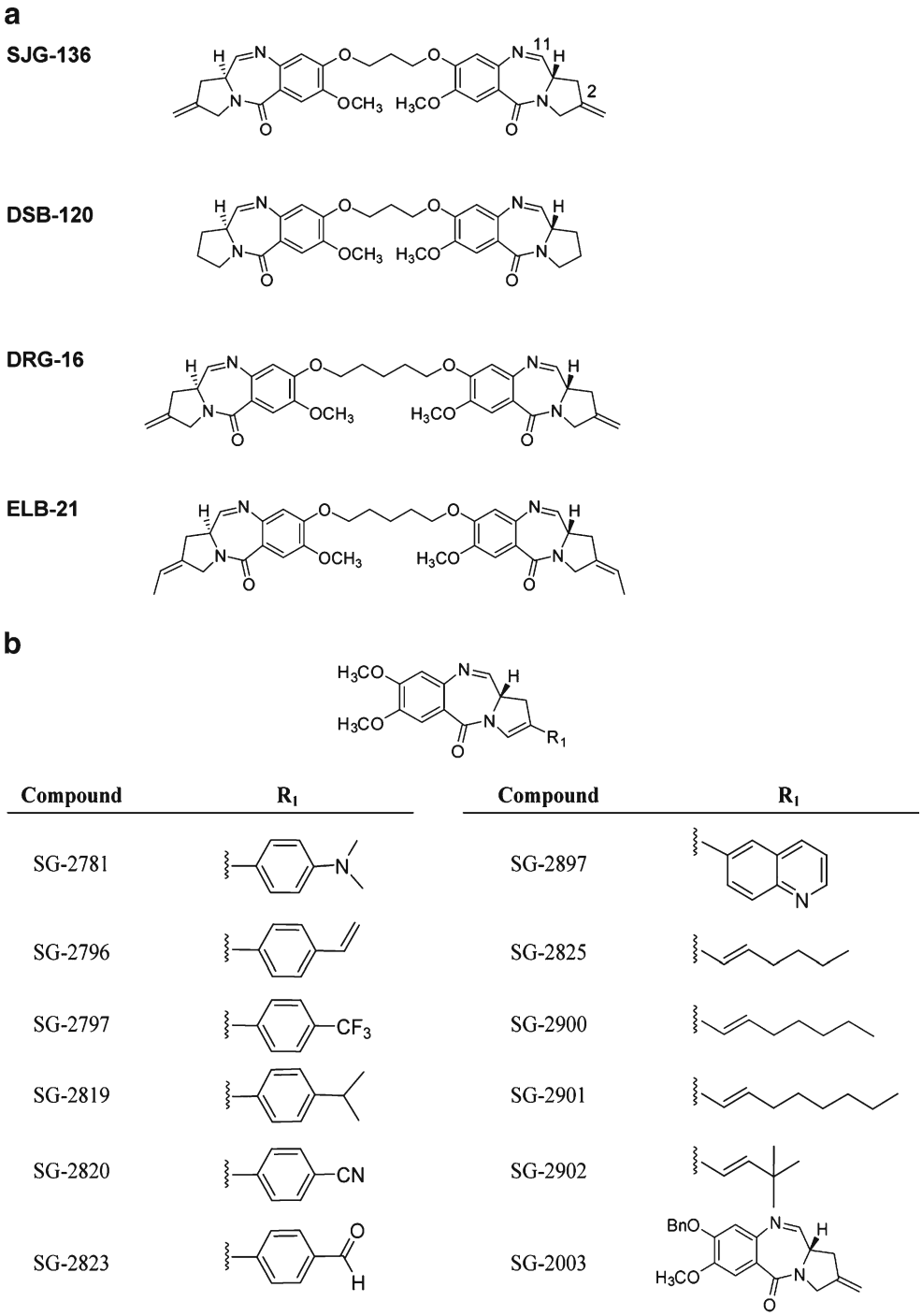

Fig. 1. Chemical structure of PBD dimers (**a**) and PBD monomers (**b**) analogs investigated. The carbons C2 the C11 have been marked for reference in the text

The isogenic cell lines used in the first experiment express nonphysiological levels of the transporters. Additionally, resistance due to transporter expression can occur intrinsically in tumors derived from tissue normally expressing high levels of transporters (colon for example) or after exposure of cancer cells to cytotoxic agents (acquired resistance). The PBD dimers were, therefore, tested in cell lines mimicking these two situations. HCT 116 and HCT-15 are colon cancer cell lines, but only HCT-15 expresses high levels of P-gp. $A2780^{AD}$ is an ovarian cell line derived from the parental cell line A2780 and resistant to doxorubicin after *in vitro* exposure to the drug. Similarly, MCF7-MX presents an acquired resistant to mitoxantrone. The ratio of GI_{50}s between HCT 116 and HCT-15 ranged from 2.3 for DSB-120 to 7.8 for ELB-21 (Table I). The ratio of GI_{50}s in $A2780^{AD}$ and A2780 was greater than 50-fold for all PBD dimers (Fig. 2c). Resensitization was achieved by the addition of verapamil, with ratios of GI_{50}s in presence and absence of verapamil ranging from 4.2 for SJG-136 and 6.4 for DRG-16 (Fig. 2c). A similar pattern was observed for ABCG2 with a ratio of GI_{50}s

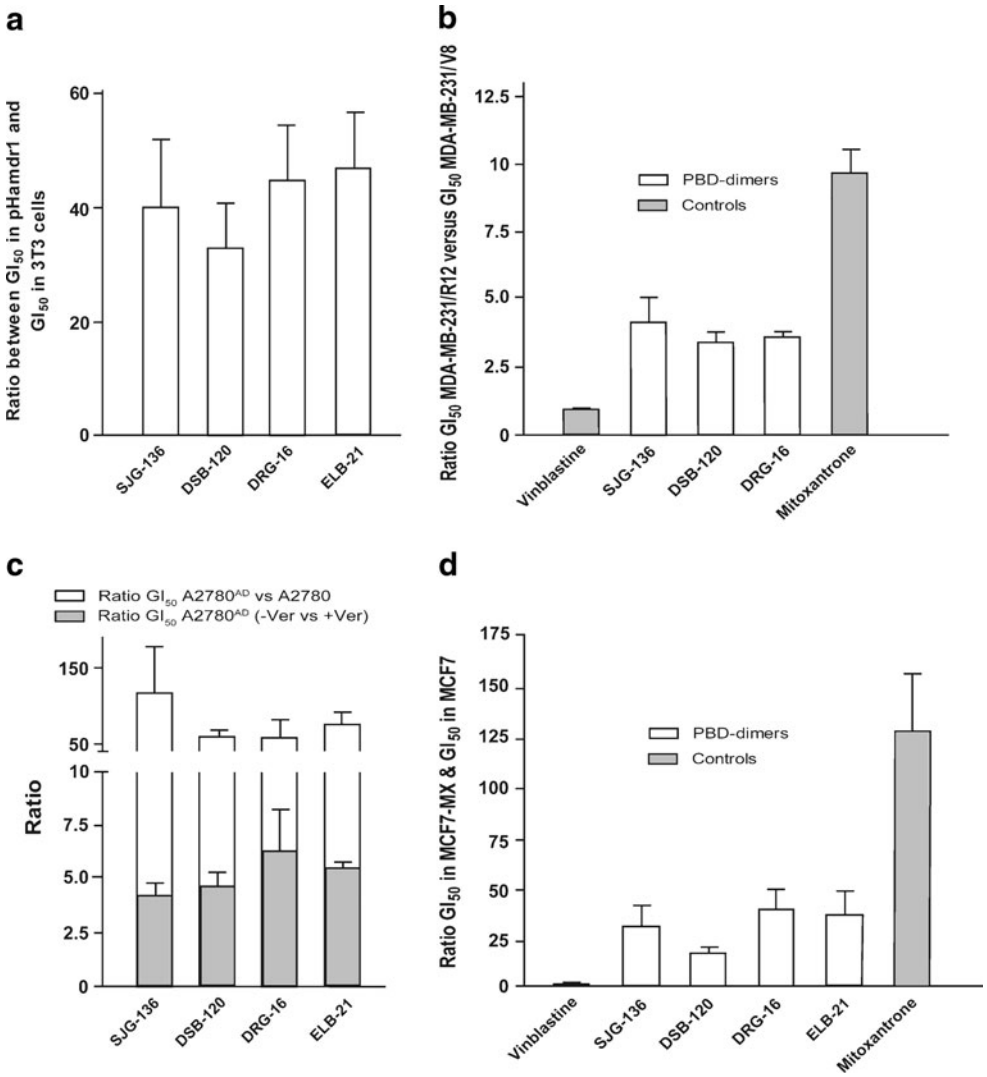

Fig. 2. Impact of ABC transporters, P-gp and ABCG2 on the growth inhibitory effect of the PBD dimers. **a** Ratios of GI_{50} in pHamdr1 cells (overexpressing P-gp) and 3T3 parental cells. **b** Ratio between the GI_{50} observed in MDA-MB-231/R12 cells, (transfected with cDNA-ABCG2) and in MDA-MB-231/V8 cells (transfected with an empty vector). Vinblastine (negative control) and mitoxantrone (positive control) are presented for comparison. **c** Impact of P-gp inhibition on the cytotoxic effect of PBD dimers in A2780 and $A2780^{AD}$. Ratio between the GI_{50} observed in A2780p and $A2780^{AD}$ (*white bars*); Ratios of GI_{50} for PBD dimers in presence and absence of verapamil in $A2780^{AD}$ (*gray bars*). **d** Ratio of GI_{50} for PBD dimers between MCF7 and MCF7-MX. All results are mean of ratios ± SEM of at least three experiments performed in triplicate

Table I. Sensitivity of HCT 116 and HCT-15 Cells to Pyrrolobenzodiazepine Derivatives

	HCT 116		HCT-15		Ratios GI_{50} HCT-15 and GI_{50} HCT 116[a]	
	GI_{50} (nM)	SD	GI_{50} (nM)	SD	Ratios	SD
SJG-136	0.72	0.24	2.5	0.46	3.6	0.1
DSB-120	42	18	85	32	2.3	1
DRG-16	0.044	0.015	0.22	0.09	5.5	2
ELB-21	0.026	0.01	0.19	0.12	7.8	1

[a] Ratios between the GI_{50} in HCT-15 cells and the GI_{50} in HCT 116 cells are expressed as means between independent experiments. Results are means of at least three independent experiments performed in triplicate

in MCF7-MX compared to MCF7 greater than 30 for all PBD dimers (Fig. 2d). ABCG2 substrate specificity of the PBD dimers was confirmed using FTC, a specific inhibitor of the transporter (Supplementary data S1). Overall, PBD dimers tested in these different cell lines show a reduced cytotoxic effect in cell lines expressing high levels of P-gp or ABCG2.

PBD dimers crosslink the DNA and induce the formation of γH2AX foci at sites of DNA damage. To confirm that expression of P-gp had a direct impact of the ability of PBD dimers to exert their mechanism of action, the presence of γH2AX foci was determined in A2780 and A2780^{AD} cells in presence of DRG-16 ± verapamil (P-gp blocker). In A2780^{AD} cells, low levels of γH2AX foci were observed after exposure to DRG-16. A 2-fold increase in the number of γH2AX foci was observed in cells exposed to DRG-16 in presence of verapamil (Fig. 3a and b). In A2780 cells, exposure to DRG-16 induced a dose- and time-dependent formation of γH2AX foci (data not shown).

Finally, the direct impact of the transporters on the PBD dimers was assessed by measuring the permeability of two PBD dimers SJG-136 and DRG-16 across a monolayer of differentiated Caco-2 cells, the most extensively characterized cell-based model to examine the permeability of drugs (Fig. 3c). The permeability was measured from the apical to the basal side (P*app* $_{A\rightarrow B}$) and from the basal to the apical side (P*app* $_{B\rightarrow A}$). Both SJG-136 and DRG-16 show an efflux

Fig. 4. Impact of MRP1 on the cytotoxic effect of PBD monomers. **a** Ratio of GI_{50} for PBD monomers in A549 cells in absence or presence of MK-571. Results are means ± SEM of $n=3$ independent experiments performed in triplicate. **b** Impact of GST inhibition on the cytotoxic effect of SG-2823. A549 cells were treated with SG-2823 with (*filled triangles*, *plain line*) or without pretreatment with dicumarol (*filled squares*, *dotted line*). Results are means ± SEM idem of triplicate. **c** Impact of the inhibition of γ-glutamylcysteine synthetase on the cytotoxic effect of SG-2823. A549 cells were treated with SG-2823 with (*filled triangles*, *plain line*) or without pretreatment with BSO (*filled squares*, *dotted line*). Results are means ± SEM idem of triplicate. **d** Analysis of the conjugation of SG-2823 to glutathione *in vitro* by LC-MS. *a* Total ion chromatogram for the cell-free analysis of GSH with SG-2823. *b* Spectra taken from the peak at 3.99 min which corresponds to GSH [M+H]+308.5. *c* Spectra taken from the peak at 8.8 min which identifies the GSH conjugate [M+H]+671.5. *d* Spectra taken from the peak at 9.77 min which identifies SG-2823 [M+H]+363.5

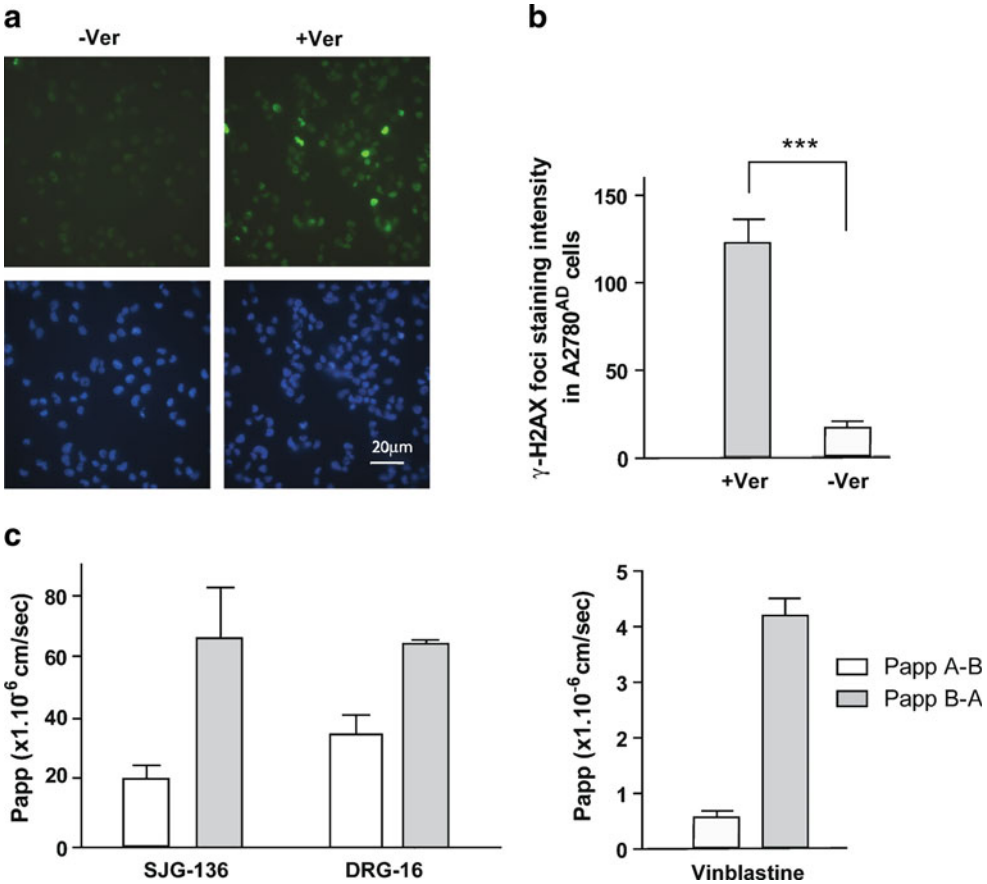

Fig. 3. Impact of the ABC transporters on DNA damage and cell permeability of PBD dimers. **a**, **b** Impact of P-gp inhibition on DNA damage observed in response to DRG-16. **a** A2780^{AD} cells were exposed to DRG-16 in presence (*left*) or absence of verapamil (*right*). Representative pictures of γH2AX foci (*top in green*). Counterstain with DAPI confirms the nuclear localisation of γH2AX foci (×40 magnification; *bottom in blue*). **b** γH2AX foci formation as expressed by staining intensity. Results are means ± SEM of 50 cells. Statistical probability is expressed as ***$p<0.001$. **c** Impact of ABC transporters on the permeability of the PBD dimers compared to P-gp substrate vinblastine as determined by the transwell assay in Caco-2 cells. *White bars* correspond to passive diffusion (Papp A→B) and *gray bars* to efflux (Papp B→A). The results are mean of ratios ± SEM of triplicate

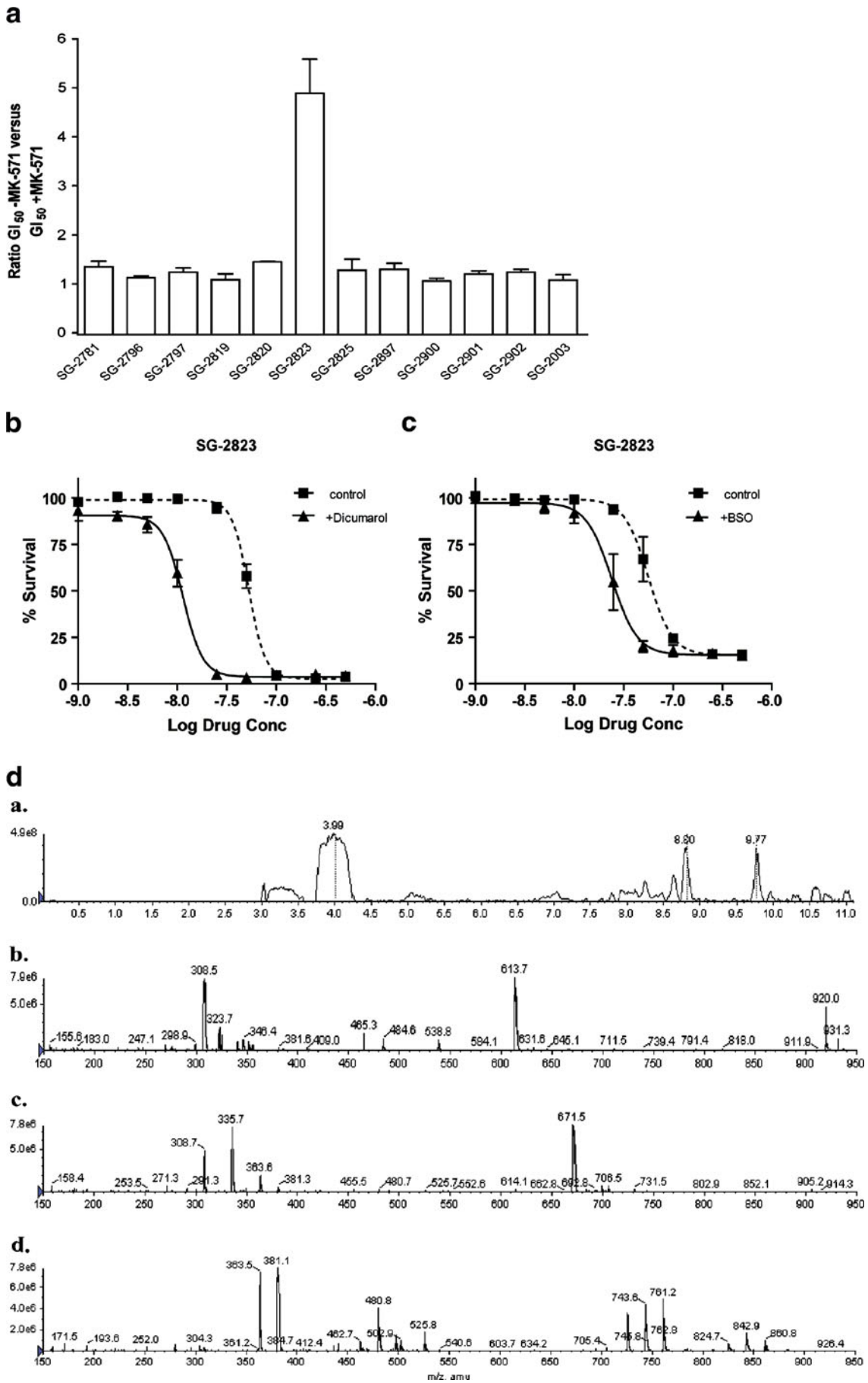
a
Ratio GI50 -MK-571 versus GI50 +MK-571
SG-2781
SG-2796
SG-2797
SG-2819
SG-2820
SG-2823
SG-2825
SG-2897
SG-2900
SG-2901
SG-2902
SG-2003
b
SG-2823
control
+Dicumarol
% Survival
Log Drug Conc
c
SG-2823
control
+BSO
% Survival
Log Drug Conc
d
a.
b.
c.
d.
m/z, amu

ratio ($Papp_{B\rightarrow A}$/ $Papp_{A\rightarrow B}$) of 6.4 for SJG-136 and 3.5 for DRG-16 consistent with both agents being actively transported by the ABC transporters.

PBD dimers, therefore, interact with ABC transporters P-gp and ABCG2. This interaction decreases the drug uptake into cancer cells, decreasing the levels of DNA crosslinks generated by PBD dimers. Decreased DNA damage translated into a reduced cytotoxic effect. Overall, it suggests that the antitumor activity of PBD dimers could be improved, provided the interaction with ABC transporters is minimized.

The PBD monomer SG-2823 Interacts with MRP1, Causing a Marked Effect on its Activity, But Only Weakly with Other ABC Transporters

The cytotoxic effect (GI_{50}) of 12 PBD monomers (Fig. 1b) were tested in the non-small cell lung cancer cell line A549, expressing high levels of MRP1 in presence or absence of a MRP1 blocker, MK-571. Pretreatment with MK-571 increased by a 5-fold factor the sensitivity of A549 cells to SG-2823 (Fig. 4a). All other PBD monomers were unaffected.

MRP1-driven transport requires a prior conjugation with glutathione via glutathione-*S*-transferase (GST). The impact of both these factors was tested. The cytotoxic effect of SG-2823 decreased when A549 cells where preincubated in presence of 100 μM dicumarol, a GST inhibitor (Fig. 4b): from 53 nM [95% confidence interval=50–55 nM] for SG-2823 alone to 11 nM [10–13 nM] in the presence of dicumarol. A549 cells were also pretreated with buthionine sulfoximine (BSO), a potent and specific inhibitor of γ-glutamylcysteine synthetase, the rate-limiting enzyme in the synthesis of GSH (26). The cytotoxic effect of SG-2823 decreased ~2.4-fold when A549 cells were pretreated with BSO: from 57 nM [95% confidence interval=50–63 nM] for SG-2823 alone to 24 nM [20–28 nM], in presence of BSO (Fig. 4c). Both dicumarol and BSO had no effect on the cytotoxic effect of another PBD monomer SG-2781 (Supplementary data S2). Finally, the formation of SG-2823 conjugated to GSH was evaluated *in vitro* and monitored by LCMS, identifying the presence of GSH, SG-2823, and GSH-SG-2823 (Fig. 4d). PBD monomers were also tested for their interaction with P-gp and ABCG2. Overall, PBD monomers were less liable to interaction with ABC transporters. However, SG-2823 interacted significantly with MRP1, decreasing its cytotoxic effect in cells expressing high levels of MRP1 and was also a weak substrate of P-gp and ABCG2 (Supplementary data S3).

Specific Physicochemical Properties of PBD Control Their Interactions with ABC Transporters

Multiple chemical features and even pharmacophores have been identified and explain, at least for some classes of compounds, their interactions with P-gp. In this study, we considered the number of nitrogen and oxygen, hydrogen bonding energy, surface activity, polar surface area, lipophilicity (Log*P*), and molecular weight (MW; Table II). The PBD dimers had a number of nitrogen and oxygen atoms (N+O) greater than 8, a hydrogen bonding energy (HBE) between 15 and 17 U, a polar surface area for all PBD dimers greater than 75 $Å^2$, all suggesting that PBD dimers had features previously identified in other P-gp substrates. Additionally, both MW and lipophilicity showed a positive correlation with the differential cytotoxicity in HCT 116 and HCT-15 cells (low and high P-gp, respectively) suggesting that lower lipophilicity and/or MW could potentially decrease the interaction with P-gp (Fig. 5a and b). Conversely, the PBD monomers had lower HBE, MW, PSA<75 $Å^2$ consistent with their weak/no interaction with P-gp. Seven out of 12 PBD monomers were surface active (Table II). However, this was not related to their differential cytotoxic effect.

To evaluate the potential interaction with ABCG2, a number of parameters relative to the hydrophilic characteristic, the electrophilic parameter and aromaticity of PBD-dimers and monomers, were tested against their relative cytotoxicity in MCF7-MX in presence and absence of FTC (ABCG2 inhibitor). Arbitrary values were attributed to

Table II. Pyrrolobenzodiazepine Derivatives Chemical Features Involved in P-gp Substrate Specificity

	MW	LogP	PSA	Hydrogen bond acceptor pattern	Hydrogen bonding energy	Basic Nitrogen	(N+O)	Surface activity	2 Aromatic rings
SJG-136	556.61	1.383	102.2	+	15	+	10	−	+
DSB-120	532.58	1.295	102.2	+	15	+	10	−	+
DRG-16	584.66	2.254	102.2	+	17	+	10	−	+
ELB-21	612.71	2.989	102.2	+	17	+	10	−	+
SG-2781	377.44	2.494	54.4	+	7.5	+	6	−	+
SG-2796	360.41	2.844	51.1	+	7.5	+	5	−	+
SG-2797	402.37	3.13	51.1	+	7.5	+	5	+	+
SG-2819	376.45	3.443	51.1	+	7.5	+	5	+	+
SG-2820	359.38	2.242	74.9	+	7.5	+	6	−	+
SG-2823	362.38	1.956	68.2	+	7.5	+	6	−	+
SG-2825	340.42	2.788	51.1	+	7.5	+	5	+	−
SG-2897	385.42	2.292	64	+	7.5	+	6	−	+
SG-2900	354.44	3.205	51.1	+	7.5	+	5	+	−
SG-2901	368.47	3.622	51.1	+	7.5	+	5	+	−
SG-2902	340.42	2.753	51.1	+	7.5	+	5	+	−
SG-2003	348.39	2.493	51.1	+	7.5	+	5	+	+

MW molecular weight; *PSA* polar surface area; (*N+O*) number of nitrogen and oxygen atoms

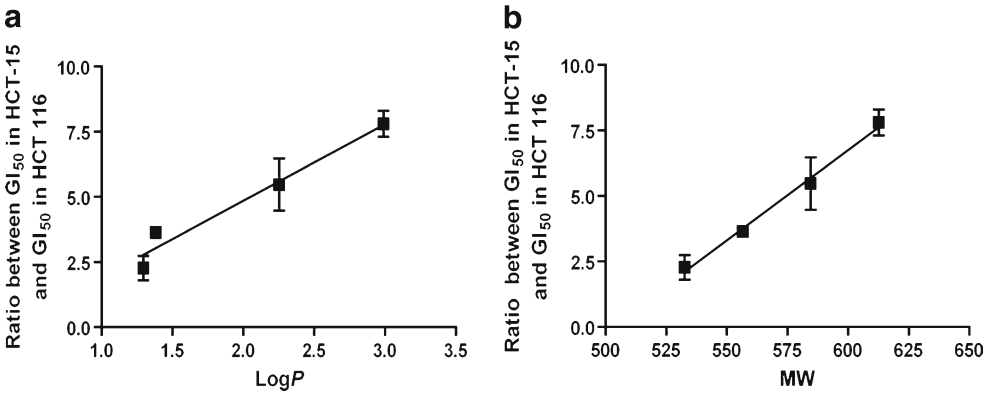

Fig. 5. Correlation between chemical features of PBD dimers and ratio of GI_{50} values in HCT 116 and HCT-15. **a** Log P; **b** molecular weight

nitrogen and oxygen atoms according to their electronegativity. The electronegativity of the fluoro groups were considered as similar as an atom of nitrogen and given an arbitrary value of 1 (the spatial distance between the different atoms of fluorine is too limited for them to make an impact as separated entities). The electrostatic potential, i.e., partial charge of the atoms, as determined by the extended Hückel calculation was also taken into consideration as well as the number of aromatic rings. The combination of all these parameters led to define the following equation (Eq. 2):

$$(n[1/2N + O]_{molecule} + n[1/2N^{-} + O^{-}]_{C2-aryl\ extremity} + n[1/2N^{-} + O^{-}]_{aromatic\ ring}) \quad (2)$$

Where $n(N^{-}+O^{-})$ is the number of oxygen atoms that are negatively charged as determined by the Hückel calculation. The equation (Eq. 2) was associated with a significant correlation with the differential cytotoxic effect in MCF7-MX (r^2=0.98; p<0.0001; Fig. 6). PBD monomers associated with a ratio −FTC *vs* +FTC<2 (SG-2796, SG-2819, 2900, SG-2901, and SG-2902) were considered as non-substrates of ABCG2 in contrast with all PBD dimers and the rest of the PBD monomers. PBD non-substrates of ABCG2 had an electrostatic potential <9 considering this value as a threshold for ABCG2 substrate specificity.

Overall, the interaction of PBDs with ABCG2 could be minimized by limiting C2 aryl substituents and the number of aromatic rings.

DISCUSSION

This study evaluated the impact of ABC transporters on a series of very potent PBD dimers and monomers and potentially avenues to minimize this interaction. The PBD dimer SJG-136 is currently in clinical development, and promising results from preclinical studies suggest that the optimization of this class of promising molecules could be highly beneficial for future drug development.

PBD dimers all had a significant interaction with ABC transporters. The analysis of the physicochemical properties responsible for this interaction highlighted MW and lipophilicity as the main factors controlling the degree of interaction. All the PBD dimers and one PBD monomer (SG-2797) had a MW greater than the accepted threshold of 400 (27), but the PBD monomer, SG-2797, was not considered to be a substrate for the ABC transporters on the basis of the biological data. However, the MW cutoff does not take into account the pK_a of the molecules. The MW cutoff would be lower for bases (28) and higher for acids (29) depending on the ionization of the compounds. PBD derivatives are weak acids (pK_a=4.1), and this study suggests that the MW cutoff for this class of compounds is likely to be higher than 400 but less than 533. Further studies with PBD monomers and dimers could be undertaken to refine this cutoff. Hydrophobicity is thought to be a major determinant in P-gp substrate specificity (1,30,31). Molecules with Log$P$<1 or >5 are predicted to be non-substrates despite having some of the physicochemical features of P-gp substrates (32). However, some of these compounds have been shown to be P-gp substrates by others (33–35). The data for the PBDs showed that although Log$P$ failed to discriminate substrates from non-substrates, it could be used to evaluate the degree of P-gp dependency, in conjunction with MW. Surface active properties, which allow the compounds to partition into the membrane and decrease the surface tension, were suggested

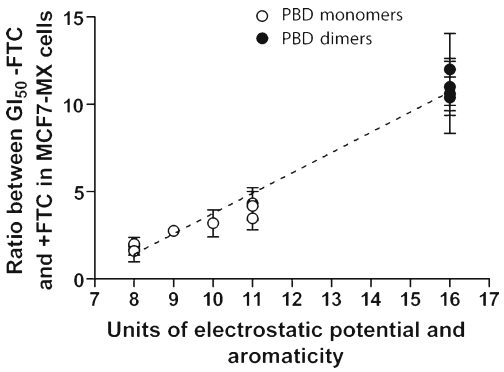

Fig. 6. Correlation between the units of electrostatic potential and aromaticity of the PBDs involved in ABCG2 substrate specificity and the ratio between the GI_{50} (FTC *versus*+FTC) in MCF7-MX cells. The electronegative potential and aromaticity was defined by the following equation $(n[1/2N + O]_{molecule} + n[1/2N^{-} + O^{-}]_{C2-aryl\ extremity} + n[1/2N^{-} + O^{-}]_{aromatic\ ring})$ where n $(N^{-}+O^{-})$ is the number of oxygen atoms that are negatively charged as determined by the Hückel calculation

to influence P-gp dependency (30). However, we found no evidence that this was the case with PBDs. All the substrates described by Seelig and Landwojtowicz were relatively basic (pK_a>7.4) and are more likely to be ionized in a relatively acid environment (30). This ionized form is traditionally thought to be membrane impermeable. The lipophilicity as described among other parameters by the surface activity could compensate and allow compounds such as PBD (when pH<pK_a) to interact with the membrane and being recognized by P-gp. Other parameters such as polar surface area, number of nitrogen and oxygen, hydrogen bonding energy, were all consistent with previous literature on P-p substrates (30,32).

The PBDs with a greater number of oxygen and nitrogen atoms and negatively charged (electrostatic potential) were associated with greater substrate specificity for ABCG2. ABCG2 substrates share a common set of physicochemical properties such as a high polarity, a greater number of aromatic rings and hydrophilic groups (36). The aromaticity of the PBDs was of interest. SG-2897 was associated with the greatest ratio (4.2) and also the greatest number of aromatic rings among the PBD monomers. However, because of its quinoline substituent, two phenomena could have had an impact on ABCG2 substrate specificity. First, the electronegative group within the ring may be the prerequisite for an enhanced interaction with the transporter. On the other hand, the electrons, organized in π orbitals, may be shared with the electrons of a surrounding planar group, thus inducing a greater interaction. This phenomenon, representing the π–π stacking interaction, as well as the electrophilic characteristic was incorporated into Eq. 2 and demonstrated a significant correlation both for the PBD dimers and PBD monomers.

Overall, this study suggests that the PBDs bind to a positively charged binding pocket of ABCG2, thus enhancing electrostatic interactions. Similar findings have been reported for a series of camptothecin analogs (36). ABCG2 is a "half transporter" which needs to homodimerize in order to be fully activated. Studies have shown that ABCG2 has at least two symmetrical binding pockets (37). PBD dimers, high affinity substrates of the transporter (potential affinity value of 16) whereas some PBD monomers, without (N+O) atoms at the C2 extremity, and being considered as the monofunctional counterpart of PBD dimers for this property, have an arbitrary potential ABCG2 affinity value of 8, half of the potential of PBD dimers. These data suggest that PBD dimers may bind to the two symmetrical binding pockets of ABCG2.

The current study provided evidence that the PBD monomer SG-2823 interacts with MRP1. The chemical structure of SG-2823 seems likely to play a major role in the ability of this compound to conjugate to GSH. SG-2823 has a carbonyl moiety at its extremity which is an electrophile, susceptible to nucleophile addition by GSH. However, the conjugate would remain highly unstable. Alternatively, the carbonyl group of SG-2823 may be involved indirectly in the coupling: it may induce a delocalization of the electrons, thus affording a greater electrophilicity of the C11. It may also attract GSH at the carbonyl without creating any bond. This induced proximity (between GSH and SG-2823) may allow the SH group to interact with C11 of SG-2823 and create a covalent bond. The mass spectrometry analysis identified the intermediate compound with a MW of 671.5 g/mol which corresponds to $[M+H]^+$ of the proposed structures. The PBDs, dimers and monomers, contain highly reactive imines in the diazepinone portions of the molecule. Cheung and colleagues have demonstrated that water or alcohol adds readily to the imino moiety of the PBD dimer SJG-136 to form the corresponding carbinolamine or its alkyl ether, respectively (38). Similar results have been demonstrated with the PBD monomers by Antonow and colleagues (personal communication). The imine of the PBDs reacts differentially with GSH, thus decreasing the potential for the entity to react with the N2 of the guanine in the minor groove of the DNA. The electrophilic centre of the PBDs at the C11 position allows these molecules to bind to DNA and exert their antitumor activity, thus limiting the electrophilic characteristic at the C2 extremity would appear to be the best strategy to limit the detoxification process mediated by GSH, GST, and MRP1.

This study, therefore, provides a clear path for further optimization: considering the MW of the building block for the PBD dimers, it is unlikely that PBD dimers will have a MW below 400. There is greater scope for the PBD monomers: a molecule, associated with a MW<402, a PSA< 75 $Å^2$, a HBE<10, an electrostatic potential <9, and lacking a carbonyl moiety at the extremity, may overcome the resistance mediated by the ABC transporters. Alternatively, the pK_a may be lowered in order to increase the thresholds such as the MW. These properties should be combined with the structural features involved in their activity (10), thus allowing a rational design of new entities with enhanced antitumor activity. As documented for other low affinity substrates, the PBD monomers would potentially be associated with an increased oral absorption and systemic bioavailability that will consequently increase the efficacy of the treatment (39–41).

ACKNOWLEDGEMENTS

Maciej Kaliszczak was a Cancer Research UK PhD student [C96/A6770], based in the Jodrell Lab, which was in receipt of Cancer Research UK Programme Grant funding [C96/A8333]. We would like to thank the Dunstaffnage Marine Laboratory (Oban, Argyll, UK) and especially Dr Tony Gutierrez for assistance in the measurement of the surface activity parameter. We would also liked to acknowledge Spirogen Ltd (London, UK) and Ipsen Ltd (Slough, UK) for providing the compounds used in this study. We thank Dr. E. Schneider (University of Maryland, MD) for providing MCF7 and MCF7-MX cell lines.

REFERENCES

1. Ambudkar SV, Dey S, Hrycyna CA, Ramachandra M, Pastan I, Gottesman MM. Biochemical, cellular, and pharmacological aspects of the multidrug transporter. Annu Rev Pharmacol Toxicol. 1999;39:361–98.
2. Silverman JA. Multidrug-resistance transporters. Pharm Biotechnol. 1999;12:353–86.
3. Deeken JF, Loscher W. The blood-brain barrier and cancer: transporters, treatment, and Trojan horses. Clin Cancer Res. 2007;13(6):1663–74.
4. Mellor HR, Callaghan R. Resistance to chemotherapy in cancer: a complex and integrated cellular response. Pharmacology. 2008;81(4):275–300.

5. Hartley JA, Spanswick VJ, Brooks N, Clingen PH, McHugh PJ, Hochhauser D, *et al*. SJG-136 (NSC 694501), a novel rationally designed DNA minor groove interstrand cross-linking agent with potent and broad spectrum antitumor activity: part 1: cellular pharmacology, *in vitro* and initial *in vivo* antitumor activity. Cancer Res. 2004;64(18):6693–9.
6. Gregson SJ, Howard PW, Hartley JA, Brooks NA, Adams LJ, Jenkins TC, *et al*. Design, synthesis, and evaluation of a novel pyrrolobenzodiazepine DNA-interactive agent with highly efficient cross-linking ability and potent cytotoxicity. J Med Chem. 2001;44(5):737–48.
7. Janjigian YY, Lee W, Kris MG, Miller VA, Krug LM, Azzoli CG, *et al*. A phase I trial of SJG-136 (NSC#694501) in advanced solid tumors. Cancer Chemother Pharmacol. 2010;65(5):833–8.
8. Alley MC, Hollingshead MG, Pacula-Cox CM, Waud WR, Hartley JA, Howard PW, *et al*. SJG-136 (NSC 694501), a novel rationally designed DNA minor groove interstrand cross-linking agent with potent and broad spectrum antitumor activity: part 2: efficacy evaluations. Cancer Res. 2004;64(18):6700–6.
9. Guichard SM, Macpherson JS, Thurston DE, Jodrell DI. Influence of P-glycoprotein expression on *in vitro* cytotoxicity and *in vivo* antitumour activity of the novel pyrrolobenzodiazepine dimer SJG-136. Eur J Cancer. 2005;41(12):1811–8.
10. Antonow D, Kaliszczak M, Kang GD, Coffils M, Tiberghien AC, Cooper N, *et al*. Structure-activity relationships of monomeric C2-aryl pyrrolo[2, 1-c][1, 4]benzodiazepine (PBD) antitumor agents. J Med Chem. 2010;53(7):2927–41.
11. Burger AM, Loadman PM, Thurston DE, Schultz R, Fiebig HH, Bibby MC. Preclinical pharmacology of the pyrrolobenzodiazepine (PBD) monomer DRH-417 (NSC 709119). J Chemother. 2007;19 (1):66–78.
12. Thurston DE. Advances in the Study of Pyrrolo[2, 1-c][1, 4] benzodiazepine (PBD) Antitumour Antibiotics: molecular aspects of anticancer drug–DNA interactions. London: Macmillan; 1993. p. 54–88.
13. Hochhauser D, Meyer T, Spanswick VJ, Wu J, Clingen PH, Loadman P, *et al*. Phase I study of sequence-selective minor groove DNA binding agent SJG-136 in patients with advanced solid tumors. Clin Cancer Res. 2009;15(6):2140–7.
14. Antonow D, Cooper N, Howard PW, Thurston DE. Parallel synthesis of a novel C2-aryl pyrrolo[2,1-c][1,4]benzodiazepine (PBD) library. J Comb Chem. 2007;9(3):437–45.
15. Gregson SJ, Howard PW, Corcoran KE, Jenkins TC, Kelland LR, Thurston DE. Synthesis of the first example of a C2–C3/C2'-C3'-endo unsaturated pyrrolo[2, 1-c][1, 4]benzodiazepine dimer. Bioorg Med Chem Lett. 2001;11(21):2859–62.
16. Louie KG, Behrens BC, Kinsella TJ, Hamilton TC, Grotzinger KR, McKoy WM, *et al*. Radiation survival parameters of antineoplastic drug-sensitive and -resistant human ovarian cancer cell lines and their modification by buthionine sulfoximine. Cancer Res. 1985;45(5):2110–5.
17. Nakagawa M, Schneider E, Dixon KH, Horton J, Kelley K, Morrow C, *et al*. Reduced intracellular drug accumulation in the absence of P-glycoprotein (mdr1) overexpression in mitoxantrone-resistant human MCF-7 breast cancer cells. Cancer Res. 1992;52 (22):6175–81.
18. Skehan P, Storeng R, Scudiero D, Monks A, McMahon J, Vistica D, *et al*. New colorimetric cytotoxicity assay for anticancer-drug screening. J Natl Cancer Inst. 1990;82(13):1107–12.
19. Artursson P, Karlsson J. Correlation between oral drug absorption in humans and apparent drug permeability coefficients in human intestinal epithelial (Caco-2) cells. Biochem Biophys Res Commun. 1991;175(3):880–5.
20. Szakacs G, Paterson JK, Ludwig JA, Booth-Genthe C, Gottesman MM. Targeting multidrug resistance in cancer. Nature reviews. 2006;5(3):219–34.
21. Hidalgo IJ, Raub TJ, Borchardt RT. Characterization of the human colon carcinoma cell line (Caco-2) as a model system for intestinal epithelial permeability. Gastroenterology. 1989;96(3):736–49.
22. Samiulla DS, Vaidyanathan VV, Arun PC, Balan G, Blaze M, Bondre S, *et al*. Rational selection of structurally diverse natural product scaffolds with favorable ADME properties for drug discovery. Mol Divers. 2005;9(1–3):131–9.
23. Burkert U, Allinger NL. Molecular MechanicsACS Monograph 177. Washington, DC: American Chemical Society; 1982.
24. Seelig A. A general pattern for substrate recognition by P-glycoprotein. Eur J Biochem. 1998;251(1–2):252–61.
25. Seelig A, Gottschlich R, Devant RM. A method to determine the ability of drugs to diffuse through the blood-brain barrier. Proc Natl Acad Sci USA. 1994;91(1):68–72.
26. Dorr RT, Liddil JD, Soble MJ. Cytotoxic effects of glutathione synthesis inhibition by L-buthionine-(SR)-sulfoximine on human and murine tumor cells. Invest New Drugs. 1986;4(4):305–13.
27. Didziapetris R, Japertas P, Avdeef A, Petrauskas A. Classification analysis of P-glycoprotein substrate specificity. J Drug Target. 2003;11(7):391–406.
28. Lee JS, Paull K, Alvarez M, Hose C, Monks A, Grever M, *et al*. Rhodamine efflux patterns predict P-glycoprotein substrates in the National Cancer Institute drug screen. Mol Pharmacol. 1994;46(4):627–38.
29. Essodaigui M, Broxterman HJ, Garnier-Suillerot A. Kinetic analysis of calcein and calcein-acetoxymethylester efflux mediated by the multidrug resistance protein and P-glycoprotein. Biochemistry. 1998;37(8):2243–50.
30. Seelig A, Landwojtowicz E. Structure-activity relationship of P-glycoprotein substrates and modifiers. Eur J Pharm Sci. 2000;12 (1):31–40.
31. Osterberg T, Norinder U. Prediction of drug transport processes using simple parameters and PLS statistics. The use of ACD/logP and ACD/ChemSketch descriptors. Eur J Pharm Sci. 2001;12 (3):327–37.
32. Varma MV, Sateesh K, Panchagnula R. Functional role of P-glycoprotein in limiting intestinal absorption of drugs: contribution of passive permeability to P-glycoprotein mediated efflux transport. Mol Pharmacol. 2005;2(1):12–21.
33. Vautier S, Lacomblez L, Chacun H, Picard V, Gimenez F, Farinotti R, *et al*. Interactions between the dopamine agonist, bromocriptine and the efflux protein, P-glycoprotein at the blood-brain barrier in the mouse. Eur J Pharm Sci. 2006;27(2–3):167–74.
34. Miyama T, Takanaga H, Matsuo H, Yamano K, Yamamoto K, Iga T, *et al*. P-glycoprotein-mediated transport of itraconazole across the blood-brain barrier. Antimicrob Agents Chemother. 1998;42(7):1738–44.
35. Mechetner E, Kyshtoobayeva A, Zonis S, Kim H, Stroup R, Garcia R, *et al*. Levels of multidrug resistance (MDR1) P-glycoprotein expression by human breast cancer correlate with *in vitro* resistance to taxol and doxorubicin. Clin Cancer Res. 1998;4 (2):389–98.
36. Nakagawa H, Saito H, Ikegami Y, Aida-Hyugaji S, Sawada S, Ishikawa T. Molecular modeling of new camptothecin analogues to circumvent ABCG2-mediated drug resistance in cancer. Cancer Lett. 2006;234(1):81–9.
37. Clark R, Kerr ID, Callaghan R. Multiple drugbinding sites on the R482G isoform of the ABCG2 transporter. Br J Pharmacol. 2006;149(5):506–15.
38. Cheung A, Struble E, He J, Yang C, Wang E, Thurston DE, *et al*. Direct liquid chromatography determination of the reactive imine SJG-136 (NSC 694501). J Chromatogr B Analyt Technol Biomed Life Sci. 2005;822(1–2):10–20.
39. Kruijtzer CM, Beijnen JH, Rosing H. ten Bokkel Huinink WW, Schot M, Jewell RC, *et al*. Increased oral bioavailability of topotecan in combination with the breast cancer resistance protein and P-glycoprotein inhibitor GF120918. J Clin Oncol. 2002;20(13):2943–50.
40. McDaid HM, Mani S, Shen HJ, Muggia F, Sonnichsen D, Horwitz SB. Validation of the pharmacodynamics of BMS-247550, an analogue of epothilone B, during a phase I clinical study. Clin Cancer Res. 2002;8(7):2035–43.
41. Bates SE, Medina-Perez WY, Kohlhagen G, Antony S, Nadjem T, Robey RW, *et al*. ABCG2 mediates differential resistance to SN-38 (7-ethyl-10-hydroxycamptothecin) and homocamptothecins. J Pharmacol Exp Ther. 2004;310(2):836–42.